Influence of Bulky Polynuclear Carcinogen Lesions in a TATA Promoter Sequence on TATA Binding Protein−DNA Complex Formation†

Olga Rechkoblit,‡ Jacek Krzeminsky,§ Shantu Amin,§ Bengt Jernström,|| Natalia Louneva,‡ and Nicholas E. Geacintov*,‡

Chemistry Department, New York University, New York, New York 10003-5180, American Health Foundation, Valhalla, New York 10595, and Division of Biochemical Toxicology, Karolinska Institute, Box 210, S-171 77 Stockholm, Sweden

Received November 3, 2000; Revised Manuscript Received February 21, 2001

ABSTRACT: The TATA binding protein (TBP) is an essential component of the transcription initiation complex that recognizes and binds to the minor groove of the TATA DNA duplex consensus sequences. The objective of this study was to determine the effect of a carcinogen-modified adenine residue, positioned site-specifically within a regulatory TATA DNA sequence, on the binding of TBP. Two 25-mer oligonucleotides with stereoisomeric 10*S* (+)-*trans*-*anti*- or 10*R* (−)-*trans*-*anti*-BPDE-N^6-dA residues at A_1 or A_2 within the TATA sequence element (5′-...TA_1TAAA...-3′)·(5′-...$TTTA_2TA$...) were synthesized (*anti*-BPDE-N^6-dA denotes an adduct formed from the reaction of *r*7,*t*8-dihydroxy-*t*9,10-epoxy-7,8,9,-10-tetrahydobenzo[*a*]pyrene). The formation of complexes with TBP of these two sequences in the double-stranded forms (1 nM) were studied employing electrophoretic mobility shift assays (EMSA) at different TBP concentrations (0−70 nM). The *overall* affinity of TBP for the BPDE-modified target DNA sequences was weakly enhanced in the case of the (+)-trans or (−)-trans lesions positioned at site A_1 with $K_d \approx 8$ and 6 nM, respectively ($K_d \approx 9$ nM for the unmodified TATA DNA). Higher-order TBP−DNA complexes were observed at TBP concentrations in excess of ∼15 nM. However, the stabilities of the biologically significant monomeric TBP−DNA complexes was dramatically increased or decreased, depending on the position of the lesion (A_1 or A_2), or on its stereochemical and conformational characteristics. A molecular docking modeling approach was employed to insert the stereoisomeric BPDE residues into the known TATA box-TBP structure [Nikolov, D. B., et al. (1996) *Proc. Natl. Acad. Sci. U.S.A.* 4862−4867] to rationalize these observations. Native gel electrophoresis experiments with the same duplexes without TBP indicate that none of the modified sequences exhibit unusual bending induced by the lesions, nor that they differ from one another in this respect. These results suggest that the hydrophobic, bulky BPDE residues influence the binding of TBP by mechanisms other than prebending. The efficiency of RNA transcription of TBP-controlled promoters could be strongly influenced by the presence of such bulky lesions that could adversely affect the levels of gene expression.

Cellular DNA is damaged by reactions with a variety of endogenous and exogenous chemicals. If the DNA lesions formed are not removed by the different repair mechanisms operative in the cell, the modified DNA can inhibit transcription or replication. Successful bypass of the lesions may result in the incorporation of the incorrect bases into the transcripts or replicated DNA strands, thus leading to mutations and cancer. Critical alterations in gene expression may also play an important role in the development of cancer. Benzo[*a*]pyrene (BP)[1] is a ubiquitous environmental pollutant that has been widely studied as a potential mutagenic and carcinogenic agent (*1*). In living cells, BP is metabolized to a variety of oxygenated derivatives, including chemically reactive and genotoxic PAH diol epoxides (*2*) that bind chemically to cellular DNA, predominantly to the exocyclic amino groups of purines. The influence of the bulky lesions derived from the binding of BP diol epoxides with DNA on the efficiency and fidelity of DNA synthesis have been extensively studied by site-directed mutagenesis methods (*3*−*5*). The BPDE-N^2-dG adducts are known to block the elongation of RNA transcripts (*6*−*8*), and the mutagenic bypass of these lesions has also been reported (*9*). The ability of DNA lesions to alter the recognition of critical DNA sequences by a number of regulatory proteins may be still another adverse effect that is beginning to receive increasing attention (*10*−*17*). MacLeod et al. (*11*) reported that BPDE-N^2-dG adducts represent high-affinity binding sites for the transcription factor Sp1. The introduction of heterologous DNA containing BPDE-adducts significantly inhibits the

† This research was supported by NIH Grant CA76660. The benzo[*a*]pyrene diol epoxides were supplied by the National Cancer Institute Carcinogen Reference Standard Repository.

* To whom correspondence should be addressed. Phone: (212) 998-8407. Fax: (212) 998-8421. E-mail: nicholas.geacintov@nyu.edu.

‡ New York University.

§ American Health Foundation.

|| Karolinska Institute.

[1] Abbreviations: BP, benzo[*a*]pyrene; BPDE or *anti*-BPDE, *r*7,*t*8-dihydroxy-*t*9,10-epoxy-7,8,9,10-tetrahydrobenzo[*a*]pyrene; TBP, TATA binding protein; DTT, dithiothreitol; EDTA, ethylenediaminetetraacetic acid; HPLC, high-performance liquid chromatography; Tris: tris-(hydroxymethyl)aminomethane; EMSA, electrophoretic mobility shift assay; PAGE, polyacrylamide gel electrophoresis.

10.1021/bi002543r CCC: $20.00
Published on Web 04/19/2001

expression of Sp1-dependent reporter genes both in vitro and in intact cells (*13*). Johnson et al. reported that the cell cycle-regulated transcription factors E2F1 and E2F4 exhibit much higher affinity for BPDE-modified DNA that contained two consensus E2F-binding sites, than for unmodified DNA of the same sequence (*12*). Vichi et al. (*14*) showed that cisplatin-treated or UV-irradiated DNA selectively attracts the promoter recognition factor TATA binding protein (TBP) and decreases transcription from TATA box containing promoters in vivo and in vitro. Although the mechanisms by which DNA lesions alter the binding affinity of these proteins are not known, many researchers suggest that a DNA bend or kink induced by the lesions enhances complex formation (*10*, *13*−*15*, *18*, *19*). Indeed, the bending of TATA promoter sequences toward the major groove by an adjacent adenine tract increases the affinity of TBP proteins for the TATA target sequence by a factor of ∼300, while a smaller extent of bending toward the major groove causes a 100-fold higher binding affinity (*20*). Enhancing the flexibility of the binding sites of TBP, which itself kinks the DNA, enhances the affinity of TBP more than 100-fold, and the TBP−DNA complex is stabilized (*21*). However, the presence of a bend induced by a single site-specific BPDE-N^2-dG adduct at the central dG residue of a GC box recognition sequence, can abolish Sp1 binding (*10*). Furthermore, a BPDE-N^2-dG adduct positioned within the binding site of an AP-1 transcription factor decreases the binding of AP-1 by approximately 50% (*22*).

The TATA binding protein (TBP) is a key transcription factor and an essential component for transcription initiation by all three nuclear RNA polymerases (*23*). In RNA polymerase II genes, TBP is part of the general transcription factor TFIID. It first binds to the TATA box and then recruits the other factors including RNA polymerase that are required for transcription (reviewed in ref *24*). On the basis of electron microscopy measurements of the human TFIID-IIA−IIB complex, it was shown that TBP is located between TFIIA and TFIIB at the top of the cavity that encompasses the TATA DNA binding region of the supramolecular complex (*25*). In RNA pol III genes, TBP is part of TFIIIB and is required for transcription of the TATA-less genes as well as for the transcription of the yeast SNR6 gene which does contain a TATA box (reviewed in ref *26*). Crystallographic studies have shown that the TBP residues make contact with 8 base pairs in the minor groove of the TATA elements and dramatically alter the DNA structure (reviewed in ref *24*). The DNA duplex is unwound by 120°and the duplex is bent at a sharp angle with a concomitant widening of the minor groove.

The first step in the assembly of a transcriptional complex is the binding of TBP to DNA (*24*). Transcription of RNA by pol II and pol III from promoters containing the TATA boxes is believed to correlate with (1) the rate of TBP association with the promoter and (2) the stability of the TBP−TATA DNA complexes (*21*, *27*−*30*). The TBP−DNA cocrystal structure (reviewed in ref *24*), and the kinetics of TBP binding to DNA (*27*−*29*, *31*−*33*) are well established. Thus, TBP is a useful model protein for studying the effect of DNA lesions on the binding of a transcription factor to DNA, and thus to elucidate the potential impact of bulky hydrophobic lesions on transcription.

Scheme 1: Structures of the (+)-*trans*- and (−)-*trans*-*anti*-BPDE-N^6-dA Adducts[a]

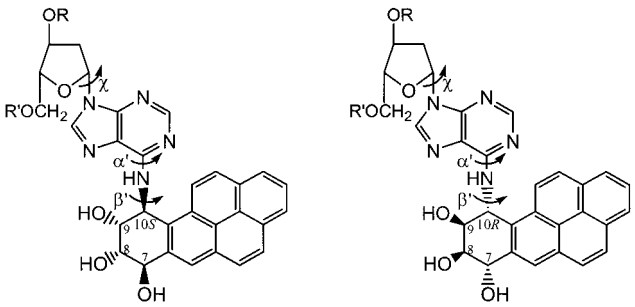

10*S* (+)-*trans*-*anti*-BPDE-N^6-dA 10*R* (-)-*trans*-*anti*-BPDE-N^6-dA

[a] Torsion angles χ, α', β' are defined as shown.

Scheme 2: TBP recognition sequence

```
[A1]  5′-GAATTCCGT[A*]T-AAATACGTGTCGTG-3′
      3′-CTTAAGGCA-T--A-TTTATGCACAGCAC-5′

[A2]  5′-GAATTCCGT-A--T-AAATACGTGTCGTG-3′
      3′-CTTAAGGCA-T[A*]TTTATGCACAGCAC-5′
```

[a] **[A*]** denotes either an unmodified dA residue, or a BPDE-modified dA residue. The abbreviation [A_1], [A_2] represents a TATA DNA duplex with a (+)-*trans*-, or (−)-*trans*-*anti*-BPDE-N^6-dA residue at the position A_1 or A_2. The TBP target sequence is shown in bold.

Earlier work has shown that transcription of DNA sequences containing site-specific BPDE-N^2-dG adducts catalyzed by various RNA polymerases can be adversely affected by these lesions (*7*, *8*). The question remains whether the initial TATA box recognition step by TBP is also affected by BPDE−DNA adducts, thus impacting on the initiation step of the transcription process itself. In this work, we have synthesized four site-specific adducts derived from the binding of the mutagenic and tumorigenic BP diol epoxide stereoisomers (+)- and (−)-*r*7,*t*8-dihydroxy-*t*9,10-epoxy-7,8,9,10-tetrahydrobenzo[*a*]pyrene (*anti*-BPDE) to the N^6 group of 2′-deoxyadenosine residues (Scheme 1) in the TATA recognition sequence 5′-d(...TA_1TA...)•5′−d(...TA_2-TA...). The (+)- and (−)-adducts are positioned at either A_1 or A_2 embedded in a 25-mer oligonucleotide duplex sequence (Scheme 2). These two adenine sites were selected for modification because they are the two most conserved adenine residues in the TBP recognition box, and are found in most TATA box sequences. In fact, 83.4 and 88.8% of eukaryotic RNA pol II promoter elements contain adenine at the A_1 and A_2 sites, respectively (*34*).

The binding of the human TATA binding protein TBP to each of these modified sequences and to unmodified DNA was compared. We find that, depending on the adduct stereochemistry and position of the lesion on one strand or the other, the biologically important 1:1 complex of TBP and the TATA box DNA sequence, is either enhanced or abolished entirely.

MATERIALS AND METHODS

Materials. HPLC-grade acetonitrile, methanol and distilled water were purchased from Fisher Chemicals. [γ-^{32}P]ATP (specific activity, >5000 Ci/mmol) was obtained from NEN LifeScience Products, Inc. The human TATA binding protein (TBP) was obtained from Promega Corp. TBP was determined to be 25% active for TATA DNA binding by titration of the TATA oligonucleotide duplexes (40 nM) with the

protein, as described (*31*). The T4 polynucleotide kinase was purchased form Amersham Life Sciences, Inc.

Synthesis of Modified Oligonucleotides. The modified oligonucleotides were synthesized by automated DNA synthesis methods employing the appropriate phosphoramidite derivatives using slightly modified published methods. The fluorinated 2′-deoxypurine nucleoside was prepared as described by Robins and Bason (*35*) and the method of Lakshman et al. (*36*) was used for bis-silylation to afford 6-fluoro-9-(2′-deoxy-3′,5′-bis(*tert*-butyldimethylsilyl)-β-D-erythropentafuranosyl) purine in 93% yield. The (±)-10β-amino-7β,8α,9α-trihydroxy-7,8,9,10-tetrahydrobenzo[*a*]pyrene was prepared by aminolysis of the corresponding (±)-*anti*-diol epoxide as described by Kim et al. (*37*) using a modified approach (after aminolysis, the aminotriol product was precipitated with cold methanol and filtered, yielding white crystals of good purity). Coupling of 3′,5′-bis-O(*tert*-butyldimethylsilyl) derivative of 6-fluoro-9-(2-deoxy-β-D-*erythro*-pentafuranosyl)purine with the (±)-10β-amino-7β,8α,9α-trihydroxy-7,8,9,10-tetrahydrobenzo[*a*]pyrene, in the presence of hexamethyldisiloxane in DMF:2,6-lutidine (*38*) at 90−100° C for 40 h, resulted in the formation of pairs of diastereomeric adducts. The subsequent synthetic steps were similar to those described previously (*37*−*39*) with minor modifications. The BPDE adducts obtained from the coupling reactions were acetylated in pyridine to give (±)-N^6-[10β-(7β,8α,9α-triacetoxy-7,8,9,10-tetrahydrobenzo-[*a*]pyrenyl)]-3′,5′-bis(*tert*-butyldimethylsilyl)-2′-deoxyadenosine with an overall yield of 67%. The desilylation with tetrabutylammonium fluoride in THF gave unprotected carbohydrate 3′- and 5′-hydroxyls, and yields of ∼80% were obtained after protection of the 5′-position. Phosphitylation of the protected adducts with 2-cyanoethyl-*N*,*N*-diisopropylchlorophosphoramidite in the presence of *N*,*N*-diisopropylethylamine gave the desired (±)-3′-phosphoramidites (±)-N^6-[10β-(7β,8α,9α-triacetoxy-7,8,9,10-tetrahydrobenzo-[*a*]pyrenyl)]-3′[(*N*,*N*-diisopropylamino)(2-cyanoethoxy)-phosphinyl]-5′-(4,4′-dimethoxytrityl)-2′-deoxy-adenosine in 74% yield. After deprotection, the two oligonucleotides with single [A*] = 10*R* (−)-and 10*S* (+)-*trans*-*anti*-BPDE-N^6-dA (Schemes 1 and 2) lesions were separated from one another using reverse phase HPLC methods as described earlier (*40*).

Measurement of the TBP Binding Affinity. The TBP−DNA complex stability was determined using an electrophoretic gel mobility shift assay (EMSA). The primer strands were labeled at the 5′-end using T4 polynucleotide kinase and [γ-^{32}P]ATP, and then purified using denaturing 20% polyacrylamide gel electrophoresis (PAGE) containing 7 M urea. The unmodified and BPDE-N^6-dA modified DNA duplexes were prepared by annealing the single strands (2-fold excess of the unlabeled strand), and heating the solution to 90 °C, followed by slow cooling to room temperature. For a typical experiment, 3 μL of the TBP solution were added to 7 μL of the DNA duplex solution. The DNA double strand concentrations used in the experiments were about 1 nM. The TBP concentrations in the reaction mixtures were varied from 0.9 to 70 nM. Solutions containing the TBP−DNA complexes were incubated for 20 min at room temperature followed by 15 min at 4 °C in 20 mM Tris-HCl (pH 8.0), 10 mM $MgCl_2$, 80 mM KCl, 8 mM DTT, 10% (v/v) glycerol, and loaded into a 4% native polyacrylamide gel (60:1 acrylamide to bis-acrylamide). The running buffer was 45 mM Tris borate, 4 mM $MgCl_2$, 0.5 mM EDTA, 0.02% NP-40. The samples were electrophoresed at 9 V/cm for 2 h at 4 °C. The gel was subsequently dried, exposed to an imaging plate, and analyzed quantitatively using a BioRad GS-525 PhosphorImager scanner.

Comparison of the Electrophoretic Mobilities of Protein-Free DNA Duplexes. Seven μL of 10 nM solutions of the unmodified and BPDE-N^6-dA modified DNA duplexes, prepared by annealing the single strands (25% fold excess of the unlabeled strand) as described above, were loaded into 8% native polyacrylamide gel (29:1 acrylamide to bis-acrylamide). Electrophoresis was performed at 3.5 V/cm for 18 h at 4 °C in 45 mM Tris borate, 0.5 mM EDTA. The gel was then dried and analyzed as mentioned above.

Measurements of DNA Duplex Melting Curves. The concentrations of the double stranded DNA were approximately 4 μM. The unmodified complementary strands were in 10% excess over the BPDE-modified single-stranded oligonucleotides. All samples were dissolved in 20 mM Na_2HPO_4 (pH 7.0), 100 mM NaCl buffer solutions. The DNA melting curves were monitored by measuring the absorption spectra of the solutions while the temperature was increased at a rate of 1 °C/min. At each temperature, the temperature was maintained for 25 s before the full absorption spectra were recorded employing an Hewlett-Packard UV−vis spectrophotometer equipped with a temperature controller. The DNA absorbance at 260 nm and the BPDE adduct absorbance at 352 nm were plotted as a function of temperature. The melting points were calculated from the maximum in the first derivative of the absorbance vs temperature plots.

Molecular Modeling. To gain insights into the fit of the bulky BPDE residues in the TBP−DNA complexes, we docked the (+)- or (−)-*trans*-BPDE moieties at A_1 or A_2 to the TATA box DNA (see Scheme 2) within a human TBP−DNA complex of known structure (*41*). The coordinates of the TBP−DNA complex were obtained from the Protein Data Bank, structure ID 1CDW, and visualized using Insight II software (Molecular Simulations Inc., a subsidiary of Pharmacopeia, Inc). The coordinates of the (+)- and (−)-*trans*-BPDE-N^6-dA moieties were those of Tan et al. (*42*). The covalent bond between the C10 atom of the BPDE residue and the N^6 atom of the adenine residues at sites A_1 or A_2 was created for both BPDE stereoisomers by using the biopolymer module of Insight II. The torsion angles α′, β′, and χ (see Scheme 1) were changed manually and kept within the bounds of the energetically acceptable range (*42*), all other parameters of the protein−DNA complex were held constant. The best TBP/BPDE-N^6-dA TATA DNA structures were selected on the basis of the least disturbance of the original structure of the unmodified TBP−DNA complex (*41*). Energetically unacceptable steric clashes were monitored by using the appropriate modular option of Insight II.

RESULTS

DNA Substrate Design. The influence of the bulky stereoisomeric BPDE residues (Scheme 1) on the binding of a recombinant human TBP transcription factor to the TATA box DNA sequences was studied using unmodified and BPDE-dA modified DNA duplexes. The BPDE-N^6-dA

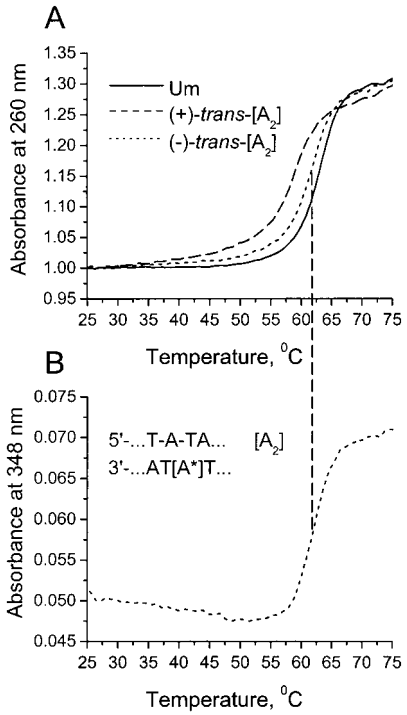

FIGURE 1: UV melting profiles at 260 nm for unmodified, (+)-*trans*- and (−)-*trans*-BPDE-N^6-[A_2] duplexes (panel A). (B) UV melting profile at 348 nm of the (−)-*trans*-BPDE-N^6-[A_2] duplex.

Table 1: Unmodified and *BPDE*-N^6-dA Modified Double Strand DNA Melting Points

DNA duplex	melting point (°C)
unmodified	63.0 ± 0.5
10*S* (+)-*trans*-[A_1]	60.0 ± 0.5
10*R* (−)-*trans*-[A_1]	63.0 ± 0.5
10*S* (+)-*trans*-[A_2]	58.7 ± 0.5
10*R* (−)-*trans*-[A_2]	62.0 ± 0.5

lesions were positioned within the consensus human TBP recognition sequence (5′-...TA_1TAAA...-3′)•(5′-...TTTA_2-TA...) embedded within a 25-mer oligonucleotide (Scheme 2), where the subscripts 1 and 2 designate the BPDE-modified adenine residues. Transcription from such a promoter sequence (without the BPDE residues) is highly efficient using HeLa cell extracts in vitro and in vivo (*43*). Four different modified oligonucleotides were prepared with A_1 (or A_2) = (+)-*trans*- or (−)-*trans*-BPDE-N^6-dA (Scheme 1).

Thermodynamic Stabilities of the TATA Box BPDE-Modified Duplexes. It is important to probe the integrity of the duplexes containing the BPDE-N^6-dA lesions since these kinds of lesions are known to thermodynamically destabilize double-stranded DNA in an adduct stereochemistry-dependent and DNA sequence-dependent manner (*44*−*47*). Typical melting profiles, obtained by monitoring the UV absorbance of the samples at 260 nm, are shown in Figure 1 (panel A). The duplex melting point, T_m, values of the duplexes derived from the unmodified and BPDE-modified oligonucleotides are compared to one another and to unmodified duplexes in Table 1. The T_m of the unmodified duplex studied here is 63 ± 0.5 °C. The same duplexes with the 10*R* (−)-trans adducts at either of the two positions exhibit the same T_m values within experimental error. However, a ∼3−4 degree lowering in the T_m values is observed in the case of the

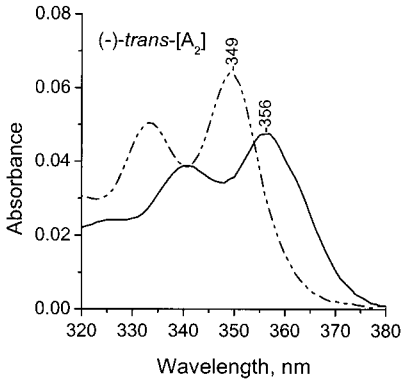

FIGURE 2: Absorption spectra in the 320−380 nm wavelength range of (−)-*trans*-BPDE-N^6-[A_2] duplex before (at 25 °C, straight line) and after (at 75 °C, dotted line) thermal denaturation. (− - - −) Denatured, 75 °C; (—) double stranded, 25 °C.

duplexes with the 10*S* (+)-trans adducts. These differences follow the trends established for the analogous lesions in much shorter, 9−11-mer duplexes (*45*−*47*). The differences in the T_m values are more pronounced in the case of the smaller duplexes (*45*−*47*), as expected. Since the ratio of normal base pairs/adduct is much larger in the 25-mers than in the 9−11-mers, the overall effect of the lesions on the T_m value is expected to be much smaller in the case of the longer sequences. It is therefore important to monitor the local melting of the duplex in the immediate vicinity of the adduct, i.e., within the absorption band of the aromatic BPDE residue. The absorption spectra of the adducts in double-stranded DNA at 25 °C, and of the denatured, single-stranded form at 75 °C, are compared in Figure 2. In double-stranded DNA, the aromatic pyrenyl ring system of the BPDE-N^6-dA adducts is intercalated (*45*), thus accounting for the red-shifted and weaker absorption spectrum of the pyrenyl residue in the ∼320−380 nm region (*48*). As the temperature is increased, the absorbance at 349 nm increases due to a hyperchromic effect as the carcinogen-DNA base stacking interactions are weakened (Figure 2), and the absorption maximum shifts from 356 to 349 nm. Thus, the changes in the absorption spectrum in the ∼343−352 nm are suitable for monitoring local denaturation at the site of the lesion (*46*). A typical melting curve for a (−)-trans adduct at the A_2 site is shown in panel B of Figure 1. The shapes of the melting curves measured at 348 nm, or within the DNA region at 260 nm, are similar to one another, and the T_m values coincide within experimental error. Therefore, the modified DNA duplexes melt cooperatively and the lesion does not cause any local premelting or unusual local destabilization of the duplexes.

Electrophoretic Mobilities of BPDE-Modified TATA Box DNA Duplexes. In the polyacrylamide gels employed to study the binding of TBP to DNA, both the unmodified and the BPDE-modified DNA duplexes are stable. This is shown by the electrophoretic migration of the carcinogen-modified duplexes that migrate as single bands in a native gel (Figure 3). Any dissociation of the duplexes would have been noticeable since the single-stranded oligonucleotides migrate with a mobility that is ∼10% slower than that of the BPDE-modified single strands (data not shown). The modified TATA 25-mer duplexes with the lesions positioned at either base A_1 or A_2 (Scheme 2), migrate with a mobility about 1% smaller than the mobility of the unmodified duplexes

FIGURE 3: Comparison of electrophoretic mobilities of unmodified and (+)-*trans*- [(+)-*t*] or (−)-*trans*- [(−)-*t*] BPDE-N^6-dA modified [A_1] and [A_2] duplexes in 8% native polyacrylamide gels.

(Figure 3). These small differences in electrophoretic mobilities of the BPDE-modified and unmodified duplexes suggest that bending effects associated with the adducts are not very pronounced. This conclusion is reasonable since a small bending angle of the order of ∼10° for (+)-*trans*-*anti*-BPDE-N^6-dA adducts was reported by Le et al. (*49*), although in a different sequence context.

Formation of TBP/Unmodified TATA DNA Complexes. The results of typical gel mobility shift experiments performed at constant concentrations of double stranded DNA (1 nM) and at different protein concentrations, are shown in Figure 4.

The slow dissociation of the human TBP dimers is known to limit the rate of binding of monomeric TBP to DNA (*32*, *50*). The TBP dimers dissociate rather slowly ($t_{1/2}$ = 6−10 min), and the efficiency of TBP binding to DNA, measured by a filter retention assay, reaches saturation after ∼15−30 min, depending on the TBP concentration. Binding is complete after 6−10 min of TBP incubation with TATA DNA at TBP concentration 10 nM, as shown by the digestion of the TBP−DNA complexes by DNAse I (*27*). Our TBP−DNA solutions were therefore incubated for 30 min before the samples were loaded onto the gels. Longer incubation times were avoided because of the possibility that TBP might denaturate (*33*).

As the TBP concentration is increased, the intensity of the lower band, which corresponds to the free DNA duplex (the band labeled D in Figure 4A), diminishes and the upper, slower running band associated with the TBP monomer−DNA complexes appears (band M in Figure 4A). This band is partially smeared because of the dissociation of the 1:1 TBP−DNA complexes during electrophoresis. Analogous binding patterns and gel electrophoresis characteristics were observed by Hoopes et al. (*27*) for yeast TBP-unmodified TATA DNA complexes. However, the human TBP-unmodified TATA DNA complexes studied here are less stable than the yeast TBP−DNA complexes studied by Hoopes et al. (*27*). The lower stabilities of human TBP−DNA complexes observed here are consistent with the results on human TBP complexes with DNA of a different sequence by others (*51*); when the EMSA method was used to examine mobilities of yeast and human TBP complexes with various plasmids under the conditions used by Hoopes et al. (*27*), considerable smearing due to the dissociation of the human TBP−DNA complexes was noted (*51*). Nevertheless, the relative mobilities of the monomeric yeast and human TBP−DNA complexes were almost identical.

Hoopes et al. (*27*) demonstrated that the rate of dissociation of the TBP−DNA complex in solution is similar to the rate observed in a 4% polyacrylamide gels. Thus, the dissociation of the TBP−DNA complexes in Figure 4 is an intrinsic solution property rather than a function of the gel environment. At TBP concentrations above 15 nM, higher order complexes become apparent (*27*). These higher-order complexes enter the gel with greater difficulty than the monomeric TBP−DNA complexes. However, only the formation of monomeric TBP−DNA complexes is believed to be biologically important, and therefore, our subsequent discussion is predominantly focused on these monomeric complexes.

Quantitative Analysis of Electrophoretic Mobility Shift Assay Data. Using the profile option of the PhosphorAnalyst program of the PhosphorImager, the relative radioactivity as a function of distance within a given lane of the electrophoresis gel was plotted. The amount of radioactive material under bands D (protein-free DNA), band M (monomeric TBP:DNA complexes) were obtained by integrating the areas under these bands, respectively. While the smearing of the bands due to the dissociation of the protein−DNA complexes and the residual radioactive material remaining in the wells of the gels (Figure 4) are not unusual (*52*−*54*), these phenomena do introduce complications into the quantitative analysis of the polyacrylamide gel autoradiographs. While the primary interest is on the concentrations of the monomeric complexes, the fractions of all complexes as a function of TBP concentration at constant DNA duplex concentration were also evaluated. Higher-order TBP:DNA complexes (see below) seem unable to enter the gel and were not included in the calculations of the fractions of TBP-bound DNA molecules. The overall fraction of DNA duplexes in complexes with proteins includes all types of TBP:DNA complexes that enter the gel from the well. This fraction corresponds to the radioactive material starting just below the well (labeled "Well" in Figure 4), divided by the overall radioactivity measured from the bottom of the well (not including the residual material in the well) to the bottom of the duplex band (labeled D in Figure 4) up to, but not including, the band due to the DNA duplexes (band D, Figure 4). The DNA molecules with slower apparent mobilities than the mobility of the free DNA band D, but faster than the DNA in monomeric complexes (band M) are attributed to DNA molecules that were initially bound to protein at the start of the electrophoresis and that dissociated during the experiment (duration ∼2 h). The fraction of DNA molecules bound as monomeric TBP−DNA complexes was estimated as the fraction of the radioactive material in band M (Figure 4) divided by the total radioactive material between the

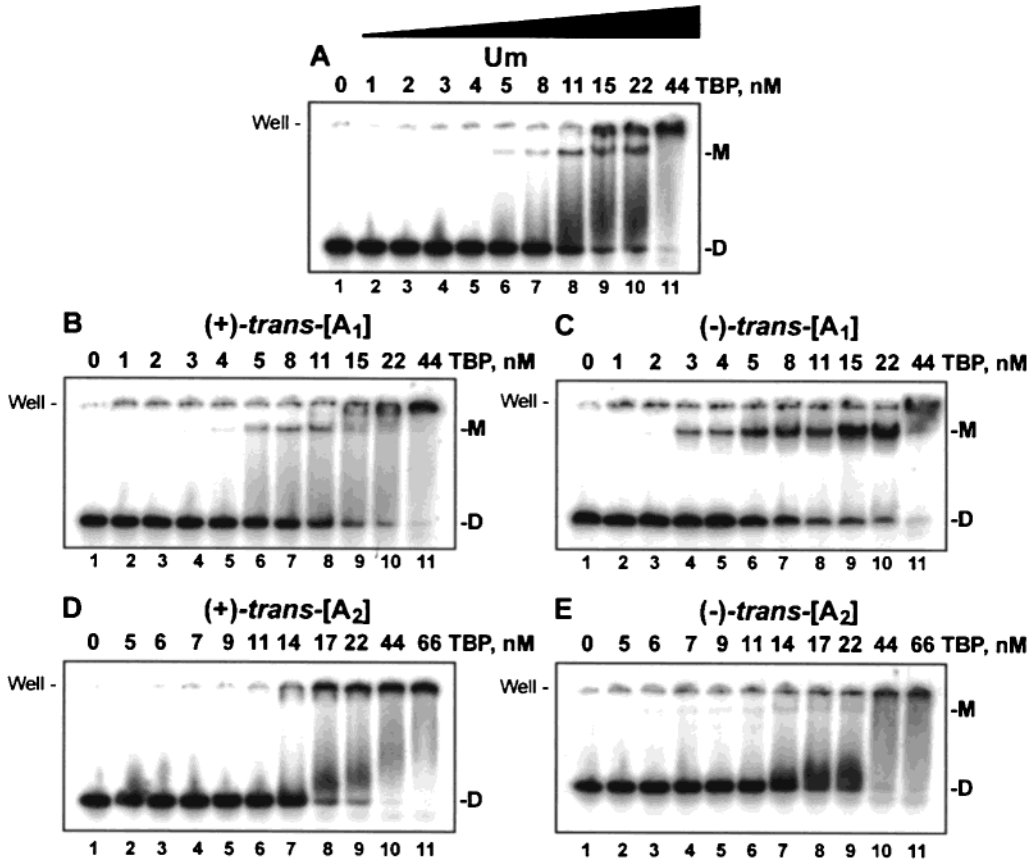

FIGURE 4: TBP complex formation with the unmodified and (+)-*trans*- or (−)-*trans*-BPDE-N^6-dA modified duplexes (1 nM) as a function of TBP concentration (0−66 nM). DNA duplexes studied are: unmodified (panel A), (+)-*trans*-[A_1] (panel B), (−)-*trans*-[A_1] (panel C), (+)-*trans*-[A_2] (panel D), (−)-*trans*-[A_2] (panel E), 4% native PAGE. Band D corresponds to the free DNA duplex, band M to the monomeric TBP:TATA DNA complex. The "Well" designates the position of the DNA or protein:DNA complexes at the start of the electrophoresis experiment.

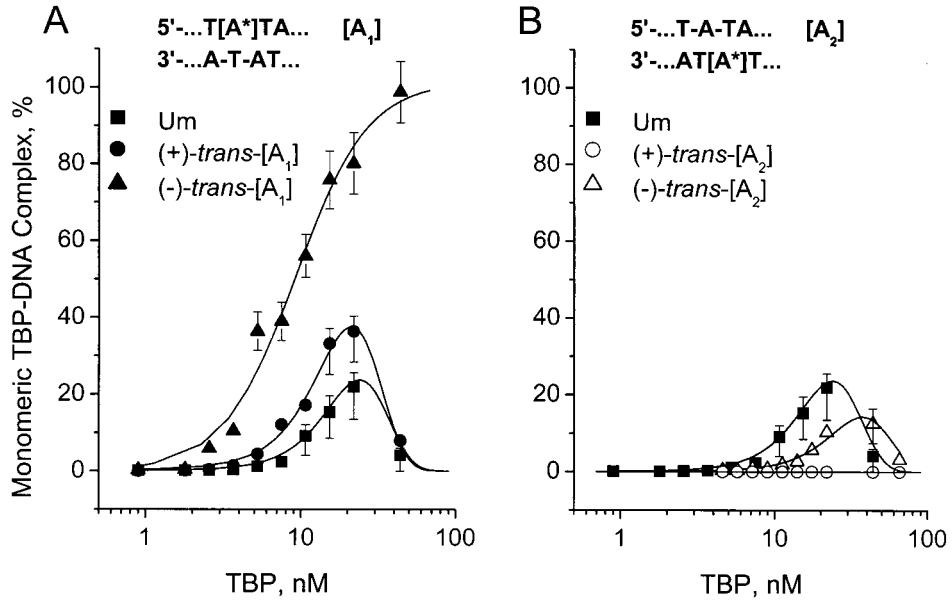

FIGURE 5: Fractions of DNA molecules bound as monomeric TBP−DNA complexes as a function of TBP concentration (band M in Figure 4). The experimental data points are represented by black squares for unmodified (Um), closed and open circles for (+)-*trans*-BPDE-N^6-dA in [A_1] or [A_2] TATA DNA duplexes, respectively. Closed and open triangles represent data for (−)-*trans*-BPDE-N^6-dA in [A_1] or [A_2] duplexes, respectively. All experimental data points represent the average of at least two separate experiments. The methods for estimating the fractions of DNA molecules bound to TBP are described in the text. The solid lines are merely visual aids and have no theoretical significance.

bottom of the well and the bottom of band D.

The fractions of monomeric complexes as a function of TBP concentration are depicted in Figure 5, while a similar plot for the overall fractions of all complexes is shown in Figure 6. Because of the complicated binding equilibria, involving formation of the monomeric and multimeric,

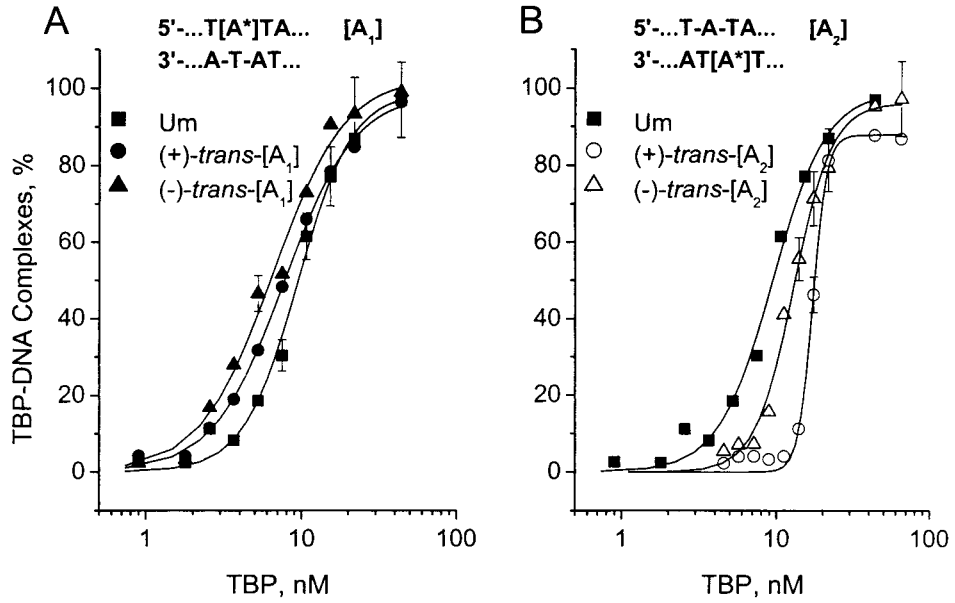

FIGURE 6: Plots of the total fractions of DNA molecules bound to TBP, entering the gels from the wells (Figure 4), as a function of TBP protein concentration. Black squares, unmodified (Um); closed and open circles, (+)-*trans*-BPDE-N^6-dA in [A_1] or [A_2] TATA DNA duplexes, respectively. Closed and open triangles, (−)-*trans*-BPDE-N^6-dA in [A_1] or [A_2] duplexes, respectively. All experimental data points represent the average of at least two separate experiments. The methods for estimating the fractions of DNA molecules bound to TBP are described in the text. The solid lines are merely visual aids and have no theoretical significance.

higher-order TBP−DNA complexes, the existence of TBP oligomers and their dissociation, and the dissociation of the TBP−DNA complexes during the gel running experiments, quantitative analysis of the binding curves is not feasible. The overall TBP−DNA complex stabilities are therefore characterized by apparent dissociation constants, K_d, corresponding to a 50% binding of the DNA molecules with TBP. The solid lines in Figures 5 and 6 merely serve as visual aids. All experimental data points represent the averages of at least two separate experiments, and the error bars denote the associated uncertainties in the quantitative estimation of fractions of TBP-bound DNA molecules.

Effects of BPDE-N^6-dA Adducts on the Formation of TBP/DNA Complexes. BPDE-Modified [A_1] Duplexes. The formation of complexes of the TATA DNA duplexes containing a single BPDE-N^6-dA residue with TBP is evident from the gel electrophoresis results shown in Figure 4. In the case of the unmodified 25-mers, as well as in the case of the (+)-trans- or (−)-trans-adducts at site A_1 (Scheme 2), monomeric, or 1:1 TBP:DNA complexes are clearly evident (band M, panels A−C, Figure 4). Some dissociation of the complexes is evident in the case of the TBP:BPDE-modified DNA duplexes (panels B and C, Figure 4), although the extent of dissociation seems to be lower than in the case of the unmodified duplexes (panel A, Figure 4). Quantitative analysis of the relevant lanes clearly indicates that the affinity of 1:1 binding of TBP with the TATA duplexes is lowest in the case of the unmodified TATA box, intermediate in the case of the A_1 = (+)-*trans-anti*-BPDE-N^6-dA, and highest when the adenine residue A_1 is substituted with the (−)-*trans-anti*-BPDE-N^6-dA lesion (Figure 5, panel A).

BPDE-Modified [A_2] Duplexes. The introduction of a (−)-*trans-anti*-BPDE-N^6-dA at adenine A_2 gives rise to a small reduction in the formation of 1:1 TBP:DNA duplexes (panel E, Figure 4, and panel B, Figure 5) relative to the unmodified duplexes. However, in the case of the stereoisomeric (+)-trans-adduct, a dramatic effect of adduct stereochemistry and adduct placement is observed since the formation of the monomeric protein:DNA complexes is completely abolished (panel D, Figure 4, and panel B, Figure 5).

Higher Order TBP:DNA Complexes. In all cases, except in the case of the (−)-trans adduct at A_1 (panel C in Figure 4 and panel A in Figure 5), the fractions of DNA molecules bound to TBP as monomeric TBP:DNA complexes generally diminishes as the TBP concentration is increased beyond ∼12−15 nM. Under the same conditions, a greater fraction of the ^{32}P-labeled DNA remains in the wells and is unable to enter the gels (upper-most bands in Figure 4), as discussed above. The formation of these higher-order TBP complexes, which trap some of the DNA in the wells and which appear at the higher protein concentration, has been previously documented (*27*, *32*), and account for the decline in the concentrations of the monomeric 1:1 TBP:DNA complexes when [TBP] > 12−25 nM (Figure 5). These higher-order complexes are attributed to complexes involving DNA regions other than TATA sequences. Using DNAse I footprinting assays, Coleman et al. (*32*) demonstrated that only the TATA box region is protected from digestion. However, at higher TBP concentrations, other DNA regions became fully covered by the protein and, at 34 nM TBP concentration, the entire DNA molecule was protected from digestion by DNAse I.

The overall extent of binding of TBP to unmodified, as well as to the BPDE-modified [A_1] and [A_2] TATA DNA duplexes is summarized in Figure 6. Dissociation constants, corresponding to a 50% concentration of free duplexes, in the range of ∼6−18 nM are estimated from these data (Table 2).

DISCUSSION

The most important step involved in eukaryotic transcription by RNA *Pol*II includes the binding of the transcription factor TFIID, a protein complex that consist of the TATA

Table 2: Complex Formation of the TATA Binding Protein (TBP) with Unmodified and BPDE-N^6-dA Modified TATA DNA Duplexes

DNA duplex	apparent dissociation constants, K_d [a] (nM)	fraction of DNA in monomeric complexes, when 50% of the DNA is bound (%)
unmodified	9 ± 2	14 ± 3
10*S* (+)-*trans*-[A_1]	8 ± 2	22 ± 4
10*R* (−)-*trans*-[A_1]	6 ± 1	65 ± 13
10*S* (+)-*trans*-[A_2]	13 ± 3	6 ± 1
10*R* (−)-*trans*-[A_2]	18 ± 3	ND[b]

[a] Apparent dissociation constants are evaluated by finding the protein concentration at which 50% of the DNA is bound (Figure 6). [b] ND, nondetected.

box binding protein (TBP) and at least seven other proteins. One of the most important mechanisms of transcription regulation of RNA *Pol*II and III activated from promoters containing TATA boxes in vivo and in vitro, is the stretch of interacting protein and DNA residues corresponding to the TATA box sequence. These interactions play a key role in determining K_d and the lifetimes of the TBP−DNA complexes (*43*, *55*).

K_d Values of TBP−DNA Complexes. Two basically different methods of determining K_d values have been employed in the field. In the first, complex formation is determined by varying the TBP concentration while holding the DNA concentration constant. In the other, the equlibrium constant is determined from measurements of the kinetic rate constants of complex formation and complex dissociation. A variety of experimental techniques are employed to measure the relevant experimental parameters. It has been suggested that, in the nanomolar TBP concentration range, the rate of complex formation is rapid, but is limited by the slow rate of dissociation of TBP dimers (*31*−*33*). Furthermore, the K_d values are known to depend strongly on the ionic strength, e.g., the concentration of KCl (*30*); for example, in the case of yeast TBP/TATA DNA complexes, $K_d \approx 1.8$ nM at 60 mM KCl, 10 nM at 80 mM KCl, and ∼100 nM at 200 mM KCl concentrations. Other values of K_d have been reported, e.g., 0.3 nM (*27*) at 60 mM KCl, 2 nM at 60 mM KCl (*56*, *57*), 4.3 nM (*28*) at 100 mM NaCl, 6.6 nM (*29*) at 100 mM KCl, 6.3 nM at 90 mM KCl (*21*), 4.2 nM at 60 mM KCl (*53*). For human TBP/TATA DNA complexes, $K_d \approx 0.5$ nM at 75 mM potassium glutamate concentrations (*31*). Our own experiments were conducted at 80 mM KCl concentrations in order to minimize the fraction of multimeric TBP−DNA complexes (*27*, *55*), and the overall concentrations of complexes were determined by the EMSA method. In the case of our unmodified TATA box DNA sequences, the apparent K_d value is ∼9 nM (Table 2), which is consistent with the range of values determined by others.

Monomeric 1:1 TBP:DNA Complexes. The values of K_d determined by most of the above-described methods refer to the formation of all forms of complexes, including monomeric and higher order TBP−DNA complexes. As described by Coleman et al. (*32*), the higher order TBP−DNA complexes consist of TBP molecules bound nonspecifically to DNA sites other then the TATA box sequences. In the absence of DNA, TBP crystallizes as a dimer (*58*). Dimers of human and yeast TBP, forming in aqueous solutions with nanomolar K_d, can also be detected in vivo (*50*). The TBP dimer interface partially overlaps with the DNA binding site (*58*), thus blocking the DNA recognition surface of TBP. In all crystallographic structures of binary TBP−TATA DNA complexes, ternary TFIIB/TBP/TATA or TFIIA/TBP/TATA complexes (for a review see ref *59*), the TBP is bound in the momomeric form. Furthermore, the three-dimensional structure of the multisubunit TFIID complex determined by electron microscopy, shows that a monomeric TBP molecule is located between the TFIIA and TFIIB proteins (*25*). It is therefore clearly of primary interest to focus on the monomeric TBP−DNA complexes (*24*) rather than on the overall binding of TBP to DNA.

Impact of Adducts on the Efficiency of the TBP−TATA Recognition Step. We chose the gel mobility shift assays for studying TBP−DNA complex formation because the monomeric complexes can be distinguished from the higher-order multimeric complexes by this method. We demonstrate that the presence of such site-specific adducts in the TATA box can have a dramatic effect on TBP binding that depends on the stereochemical properties and the position of the lesion within the TATA box sequence.

The fractions of the DNA in distinctly monomeric complexes at TBP concentrations equal to the K_ds are shown in Table 2. Since the K_d values of the monomeric TBP−TATA DNA complexes could not be measured, these fractions provide a relative measure of the efficiencies of formation of these monomeric TBP−DNA complexes. Surprisingly, the (−)-*trans*-BPDE-N^6-dA adduct in the A_1 position causes a significant increase in the stability of the monomeric complex, since its dissociation rate within the gel is significantly diminished as compared to the rate of the TBP-unmodified DNA complex (Figures 4 and 5, Table 2). In principle, a similar effect in vivo could lead to an increase in the level of transcription. Moreover, a tighter binding of the transcription factor to the lesion within the TATA sequence may prevent the recognition and excision of this sequence by DNA repair proteins (*60*).

The substitution of a dA residue in the site A_2 by a BPDE-N^6-dA adduct, especially by the (+)-*trans*-BPDE isomeric lesion, causes an increase in the dissociation rate of the monomeric TBP−DNA complex, and thus to a significant decrease in its stability (Figure 5). Such a decrease in the stability could lead to a dramatic decrease in transcriptional efficiency.

Impact of Lesions on TBP/BPDE−TATA DNA Complexes. The transcription activity, which is initiated by the binding of TBP to the d(5′-...TA_1TAAA...)·d(5′-...TTTA_2TA...) sequence, is significantly diminished when one of the base pairs in the duplex is altered (*43*). Interestingly, when the T:A_2 base is replaced by any of the other base pairs (A:T, G:C, or C:G), the reduction in the transcription activity is significantly greater than upon replacement of the A_1:T base pair. When the lesion is positioned at the site A_2, the stability of the monomeric TBP−DNA complex is much more severely affected than when the lesion is positioned at the A_1 site (Table 2). Furthermore, the stabilities of these complexes depend on the stereochemial properties of the BPDE-N^6-dA adducts.

To gain insight into these effects, we docked the (+)- or (−)-*trans*-BPDE moieties at A_1 or A_2 to the TATA box DNA in the human TBP−DNA complex of known structure (*41*), Protein Data Bank ID: 1CDW. A detailed conformational

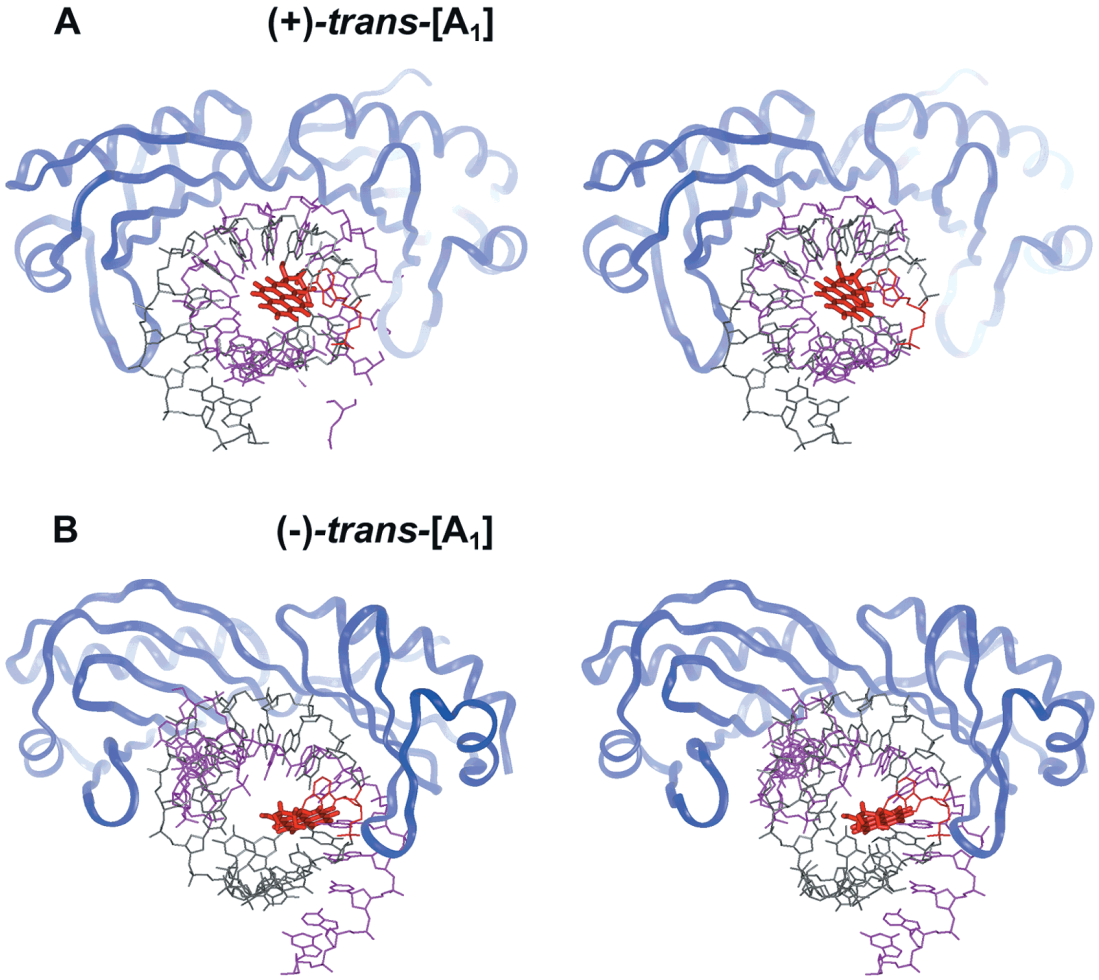

FIGURE 7: Stereoview of the complex of TBP with (+)-*trans*-BPDE-N^6-dA (A) and (−)-*trans*-BPDE-N^6-dA (B) in the A_1 position of a TATA box. The (+)-*trans* or (−)-*trans*-BPDE moieties are docked to the TBP−TATA complex of established X-ray crystal structure (*41*), Protein data bank ID: 1CDW. The TBP is depicted as a light blue ribbon. The DNA is shown in terms of a stick model. The TATA strand of the DNA duplex is shown in gray and the complementary strand is shown in magenta. The 5′ end of the TATA box is positioned on the right side, and the polynuclear (+)-*trans* and (−)-*trans*-BPDE-N^6-dA residues on the TATA strand are shown in red.

analysis of the (+)- and (−)-*trans-anti*-BPDE-N^6-dA mononucleoside adducts (Scheme 1) indicates that only four different conformational domains, each defined by a rather narrow set of torsion angles α′, β′, and χ (see Scheme 1) are energetically possible (*42*). In replacing A_1 or A_2 by any of the *trans-anti*-BPDE-N^6-dA moieties in our computer docking experiments, all of the critical protein−DNA contacts were held constant. The rationale was that an alteration in these contacts and/or conformation of the duplex within the original crystal structure of the TBP−TATA box DNA complex, would result in a distorted TBP−DNA complex conformation with a diminished stability.

In the case of the (+)-trans adduct, none of the acceptable conformational domains (*42*) could be docked successfully without altering the crystal structure of the DNA bases and/or backbone within the TATA box. Massive steric van der Waals clashes between the carcinogen and the DNA bases are observed when the adduct is at A_2. The positioning of the pyrenyl residue within the complex and within the permitted ranges of the torsion angles α′, β′, and χ of the adduct (*42*), allows for a reasonable accommodation only if some of the DNA base orientations and amino acid-DNA contacts observed in the TBP−DNA crystal structure are severely perturbed. For the (+)-trans adduct at position A_1, the aromatic pyrenyl residue can be accommodated within the cleft of the TBP−DNA complex, but there are some collisions between the aliphatic part of the BPDE residue and the first T residue of the TATA box (Figure 7A). Thus, only minor changes within the DNA portion of this complex can accommodate the lesion at A_1. The results of these simple docking exercises are consistent with the observations that the (+)-*trans-anti*-BPDE-N^6-dA lesion at position A_2 severely destabilizes the monomeric TBP−DNA complex, while a small stabilization effect is observed with the lesion at A_1. The stabilization may result from a hydrophobic displacement of water molecules out of the cleft of the TBP−DNA complex, and the concomitant entropy increase.

In the case of the (−)-*trans*-BPDE adduct, an unperturbed, or minimally perturbed TBP−DNA structure could not be found with the adduct positioned at A_2. This suggests that the complex is unstable, consistent with the experimental observations (Figure 5). However, with the lesion positioned at A_1, an adduct conformation can be identified that does not perturb the crystal TBP−DNA structure. This structure is depicted in Figure 7B and shows that the aromatic BPDE residue is positioned within the cavity of the crescent-shaped TBP−DNA complex. The torsion angles for this BPDE-N^6-dA adduct conformation ($\alpha' = 160°$, $\beta' = 90°$, $\chi = 260°$) correspond to the so-called domain III conformation (*42*). The glycosidic angle χ is within 16° of the value reported

for the same unmodified adenine nucleotide residue at position A_1 ($\chi \approx 260°$ vs $\sim 244°$ in the TBP:unmodified DNA crystal structure (*41*). There are no collisions between the BPDE residues and the DNA bases. The carcinogen appears to fit ideally into the TATA box DNA structure and does not cause any significant perturbations. However, the deoxyribose ring of the BPDE-modified adenine, which forms several contacts with the protein molecule, is somewhat closer to the TBP amino acid backbone than it is in the case of the unmodified adenine in the TBP:unmodified DNA complex crystal structure because of the slightly altered χ value. Overall, this lack of deviation of the structure of the TBP−DNA complex with a (−)-trans adduct at A_1 from the structure of the unmodified TBP:DNA complex (*41*). BPDE residue fits comfortably into the cleft of the TBP−DNA complex, thus displacing water molecules. These simple modeling results thus suggest an explanation for the observation that the (−)-*trans*-BPDE-N^6-dA adduct produces a stabilization of the TBP:DNA complex at position A_1 (Figures 4 and 5).

Role of Bending in the Recognition of Carcinogen Modified DNA by TBP. The influence of damaged or modified bases on the recognition of different DNA sequences by transcription binding factors has been the subject of considerable interest. Transcription binding proteins cause significant bending in the DNA upon complex formation as shown, for example, in Figure 7. This observation led to the hypothesis that lesions that cause significant DNA bending ("pre-bending") or increase the flexibility of the DNA target sequences, enhance the binding of transcription proteins (*20*, *21*, *53*). Thus, the presence of a bend-inducing cisplatin adduct in the vicinity of a TATA box results in a 175-fold enhancement in the binding affinity of TBP and is associated predominantly with a slower dissociation rate of the complex (*53*). Similar enhancement of TBP binding is produced by positioning a bent adenine tract adjacent to a TATA box promoter sequence (*20*). However, positioning a bend-inducing BPDE-N^2-dG adducts 6 bases upstream of the 5′-end of a TATA box, does not affect TBP binding (*61*), while the presence of a BPDE-N^2-dG adduct immediately downstream of the TATA-box caused approximately a 2-fold increase in TBP binding (Å. E. Persson, I. Voskoboinik, I. Cotgreave, and B. Jernström, private communication). The intriguing possibility that bend-inducing DNA adducts could sequester, or "hijack", transcription factors and thus adversely influence the expression of the affected genes, was the focus of a number of studies (*11*−*15*, *62*). For instance, BPDE-N^2-dG adducts are indeed high-affinity binding sites for the transcription factor Sp1 (*11*), and thus could inhibit the expression of Sp1-dependent reporter genes both in vitro and in intact cells (*13*). The E2F1 and E2F4 cell cycle-regulated transcription factors also exhibit high affinity for BPDE-modified DNA (*12*). Cisplatin-treated, or UV-irradiated DNA also exerts an enhanced affinity for the TATA binding protein (*14*). The data provided by Coin et al. (*15*) suggest that TBP binds selectively only to bend-inducing DNA adducts. The structural basis for the recognition of cisplatin-modified DNA by high-mobility-group (HMG) proteins was suggested by Ohndorf et al. (*62*). Tight binding of HMG proteins to modified DNA is achieved by a DNA kink at the platinum-DNA cross-link and intercalation of phenylalanine residues into a hydrophobic notch at the lesion site.

The effects of bulky DNA lesions within the recognition sequences of different transcription factors has also been studied. A bend-inducing BPDE -N^2-dG adduct placed within the AP-1 binding site decreased the binding an AP-1 like protein (*22*), while adducts derived from the structurally different benzo[*c*]phenanthrene diol epoxides to N^6 of adenine in DNA totally inhibited protein−DNA interactions (*61*). On the other hand, *trans*-*anti*-BPDE-N^2-dG adducts localized within the binding sequence for Oct-1 do not affect protein binding (Å. E. Persson, I. Voskoboinik, I. Cotgreave, and B. Jernström, private communication).

It is thus evident that not all types of lesion-associated bends, at least in the case of the bulky hydrophobic lesions derived from the binding of BPDE to N^2-dG, enhance the binding of TBP or other transcription factors. Such effects may be associated not only with the position of the lesion within the DNA sequence, as shown here, but also with the conformational characteristics of the lesions. The structures of site-specific BPDE-N^6-dA adducts in double-stranded oligonucleotides in different, non-TATA box sequence contexts, have been studied by various groups. The pyrenyl ring systems in both the (+)-*trans*-*anti*-adducts, with *S* and *R* absolute configurations at the C10 BPDE residue linkage site are intercalated on the 5′-side of the modified adenine residue with all Watson−Crick base pairing intact, even at the lesion site (*44*, *63*, *64*). While, it was not possible to determine a high-resolution structure with a normal T paired with the modified adenine, the pyrenyl residue in the 10*S* (+)-*trans*-*anti*-adduct is most likely intercalated on the 3′-side of the modified A*:T base pair (*65*), as it is in two A:G mismatch structures (*65*), and as discussed elsewhere (*66*). In the A_1 and A_2 TATA box sequences (Scheme 2), the NMR solution structures have not been determined. However, there is a characteristic $\sim$10 nm red shift in the 343 nm absorption band of pyrenyl residues exposed to an aqueous environment relative to 354 nm for intercalated structures in double-stranded DNA (*48*). In the two modified double-stranded TATA box sequences A_1 and A_2, the absorption spectra of all four adducts (an example is shown in Figure 2) strongly indicates that the pyrenyl ring system in the 10*S* (+)-trans- and 10*R* (−)-trans adducts are also intercalated. Furthermore, these TATA duplexes with the lesions positioned at either base A_1 or A_2, do not exhibit any anomalous electrophoretic mobilities, and all four modified sequences migrate with similar mobilities, only 1% slower as compared to unmodified DNA (Figure 3). Thus, the strikingly different impact of the stereoisomeric adducts on TBP binding, especially the enhanced binding associated with the (−)-trans adduct at position A_1, do not appear to be associated with any significant pre-bending of the sequences by the lesions. The exact reasons for these differential effects in the case of the *trans*-*anti*-BPDE-N^6-dA adducts, must be sought in the possibly more subtle changes in the interactions and changes in the structural properties of the TBP−DNA complexes with the stereoisomeric BPDE residues at either A_1 or A_2.

REFERENCES

1. Phillips, D. H. (1983) *Nature 303*, 468−72.
2. Conney, A. H. (1982) *Cancer Res. 42*, 4875−917.
3. Kozack, R., Seo, K. Y., Jelinsky, S. A., and Loechler, E. L. (2000) *Mutat. Res. 450*, 41−59.
4. Fernandes, A., Liu, T., Amin, S., Geacintov, N. E., Grollman, A. P., and Moriya, M. (1998) *Biochemistry 37*, 10164−72.

5. Page, J. E., Zajc, B., Oh-hara, T., Lakshman, M. K., Sayer, J. M., Jerina, D. M., and Dipple, A. (1998) *Biochemistry 37*, 9127−37.
6. Choi, D. J., Roth, R. B., Liu, T. M., Geacintov, N. E., and Scicchitano, D. A. (1996) *J. Mol. Biol. 264*, 213−9.
7. Choi, D. J., Marino-Alessandri, D. J., Geacintov, N. E., and Scicchitano, D. A. (1994) *Biochemistry 33*, 780−7.
8. Custer, L., Zajc, B., Sayer, J. M., Cullinane, C., Phillips, D. R., Cheh, A. M., Jerina, D. M., Bohr, V. A., and Mazur, S. J. (1999) *Biochemistry 38*, 569−81.
9. Remington, K. M., Bennett, S. E., Harris, C. M., Harris, T. M., and Bebenek, K. (1998) *J. Biol. Chem. 273*, 13170−6.
10. MacLeod, M. C., Powell, K. L., Kuzmin, V. A., Kolbanovskiy, A., and Geacintov, N. E. (1996) *Mol. Carcinog. 16*, 44−52.
11. MacLeod, M. C., Powell, K. L., and Tran, N. (1995) *Carcinogenesis 16*, 975−83.
12. Johnson, D. G., Coleman, A., Powell, K. L., and MacLeod, M. C. (1997) *Mol. Carcinog. 20*, 216−23.
13. Butler, A. P., Johnson, D. G., Kumar, A. P., Narayan, S., Wilson, S. H., and MacLeod, M. C. (1997) *Carcinogenesis 18*, 239−44.
14. Vichi, P., Coin, F., Renaud, J. P., Vermeulen, W., Hoeijmakers, J. H., Moras, D., and Egly, J. M. (1997) *EMBO J. 16*, 7444−56.
15. Coin, F., Frit, P., Viollet, B., Salles, B., and Egly, J. M. (1998) *Mol. Cell. Biol. 18*, 3907−14.
16. Zhai, X., Beckmann, H., Jantzen, H. M., and Essigmann, J. M. (1998) *Biochemistry 37*, 16307−15.
17. Chen, X. M., Gray, P. J., Cullinane, C., and Phillips, D. R. (1999) *Chem. Biol. Interact. 118*, 51−67.
18. Takahara, P. M., Frederick, C. A., and Lippard, S. J. (1996) *J. Am. Chem. Soc. 118*, 12309−21.
19. Li, G.-M., Wang, H., and Romano, L. J. (1996) *J. Biol. Chem. 271*, 24084−8.
20. Parvin, J. D., McCormick, R. J., Sharp, P. A., and Fisher, D. E. (1995) *Nature 373*, 724−7.
21. Grove, A., Galeone, A., Yu, E., Mayo, l. L., and Geiduschek, E. P. (1998) *J. Mol. Biol. 282*, 731−9.
22. Persson, Å. E., Pontén, I., Cotgreave, I., and Jernström, B. (1996) *Carcinogenesis 17*, 1963−9.
23. Hernandez, N. (1993) *Genes Dev. 7*, 1291−1308.
24. Patikoglou, G., and Burley, S. K. (1997) *Annu. Rev. Biophys. Biomol. Struct. 26*, 289−325.
25. Andel, F., III, Ladurner, A. G., Inouye, C., Tjian, R., and Nogales, E. (1999) *Science 286*, 2153−2156.
26. Geiduschek, E. P., and Kassavetis, G. A. (1995) *Curr. Opin. Cell Biol. 7*, 344−51.
27. Hoopes, B. C., LeBlanc, J. F., and Hawley, D. K. (1992) *J. Biol. Chem. 267*, 11539−47.
28. Perez-Howard, G. M., Weil, P. A., and Beechem, J. M. (1995) *Biochemistry 34*, 8005−17.
29. Parkhurst, K. M., Brenowitz, M., and Parkhurst, L. J. (1996) *Biochemistry 35*, 7459−65.
30. Petri, V., Hsieh, M., Jamison, E., and Brenowitz, M. (1998) *Biochemistry 37*, 15842−9.
31. Coleman, R. A., and Pugh, B. F. (1995) *J. Biol. Chem. 270*, 13850−9.
32. Coleman, R. A., and Pugh, B. F. (1997) *Proc. Natl. Acad. Sci. U.S.A. 94*, 7221−6.
33. Jackson-Fisher, A. J., Burma, S., Portnoy, M., Schneeweis, L. A., Coleman, R. A., Mitra, M., Chitikila, C., and Pugh, B. F. (1999) *Biochemistry 38*, 11340−8.
34. Bucher, P. (1990) *J. Mol. Biol. 212*, 563−78.
35. Robins, M. J., and Basom, G. L. (1973) *Can. J. Chem. 51*, 3161.
36. Lakshman, M. K., Sayer, J. M., and Jerina, D. M. (1991) *J. Am. Chem. Soc. 113*, 6589−94.
37. Kim, S. J., Jajoo, H. K., Kim, H. Y., Zhou, L., Horton, P., Harris, C. M., Harris, T. M., and Stone, M. P. (1995) *Bioorg. Med. Chem. 3*, 811−22.
38. Lakshman, M. K., Sayer, J. M., Yagi, H., and Jerina, D. M. (1992) *J. Org. Chem. 57*, 4585−90.
39. Steinbrecher, T., Becker, A., Stezowski, J. J., Oesch, F., and Seidel, A. (1993) *Tetrahedron. Lett. 34*, 1773−4.
40. Laryea, A., Cosman, M., Lin, J. M., Liu, T., Agarwal, R., Smirnov, S., Amin, S., Harvey, R. G., Dipple, A., and Geacintov, N. E. (1995) *Chem. Res. Toxicol. 8*, 444−54.
41. Nikolov, D. B., Chen, H., Halay, E. D., Hoffman, A., Roeder, R. G., and Burley, S. K. (1996) *Proc. Natl. Acad. Sci. U.S.A. 93*, 4862−7.
42. Tan, J., Geacintov, N. E., and Broyde, S. (2000) *J. Am. Chem. Soc. 122*, 3021−2.
43. Wobbe, C. R., and Struhl, K. (1990) *Mol. Cell. Biol. 10*, 3859−67.
44. Zegar, I. S., Kim, S. J., Johansen, T. N., Horton, P. J., Harris, C. M., Harris, T. M., and Stone, M. P. (1996) *Biochemistry 35*, 6212−4.
45. Schurter, E. J., Yeh, H. J., Sayer, J. M., Lakshman, M. K., Yagi, H., Jerina, D. M., and Gorenstein, D. G. (1995) *Biochemistry 34*, 1364−75.
46. Chaturvedi, S., and Lakshman, M. K. (1996) *Carcinogenesis 17*, 2747−52.
47. Krzeminski, J., Ni, J., Zhuang, P., Luneva, N., Amin, S., and Geacintov, N. E. (1999) *Polycycl. Aromat. Compd. 17*, 1−10.
48. Geacintov, N. E., Cosman, M., Mao, B., Alfano, A., Ibanez, V., and Harvey, R. G. (1991) *Carcinogenesis 12*, 2099−108.
49. Le, P. T., Harris, C. M., Harris, T. M., and Stone, M. P. (2000) *Chem. Res. Toxicol. 13*, 63−71.
50. Coleman, R. A., Taggart, A. K., Benjamin, L. R., and Pugh, B. F. (1995) *J. Biol. Chem. 270*, 13842−9.
51. Starr, D. B., Hoopes, B. C., and Hawley, D. K. (1995) *J. Mol. Biol. 250*, 434−46.
52. Weideman, C. A., Netter, R. C., Benjamin, L. R., McAllister, J. J., Schmiedekamp, L. A., Coleman, R. A., and Pugh, B. F. (1997) *J. Mol. Biol. 271*, 61−75.
53. Cohen, S. M., Jamieson, E. R., and Lippard, S. J. (2000) *Biochemistry 39*, 8259−65.
54. Bernues, J., Carrera, P., and Azorin, F. (1996) *Nucleic Acids Res. 24*, 2950−8.
55. Hoopes, B. C., LeBlanc, J. F., and Hawley, D. K. (1998) *J. Mol. Biol. 277*, 1015−31.
56. Imbalzano, A. N., Zaret, K. S., and Kingston, R. E. (1994) *J. Biol. Chem. 269*, 8280−6.
57. Hahn, S., Buratowski, S., Sharp, P. A., and Guarente, L. (1989) *Proc. Natl. Acad. Sci. U.S.A. 86*, 5718−22.
58. Nikolov, D. B., Hu, S. H., Lin, J., Gasch, A., Hoffmann, A., Horikoshi, M., Chua, N. H., Roeder, R. G., and Burley, S. K. (1992) *Nature 360*, 40−6.
59. Burley, S. K. (1996) *Philos. Trans. R. London B Biol. Sci. 29*, 483−9.
60. Aboussekhra, A., and Thoma, F. (1999) *EMBO J. 18*, 433−43.
61. Voskoboinik, I., Persson, Å. E., and Jernström, B. (1999) *Polycyclic Aromat. Compd. 17*, 33−42.
62. Ohndorf, U. M., Rould, M. A., He, Q., Pabo, C. O., and Lippard, S. J. (1999) *Nature 399*, 708−12.
63. Schurter, E. J., Sayer, J. M., Oh-hara, T., Yeh, H. J., Yagi, H., Luxon, B. A., Jerina, D. M., and Gorenstein, D. G. (1995) *Biochemistry 34*, 9009−20.
64. Mao, B., Gu, Z., Gorin, A., Chen, J., Hingerty, B. E., Amin, S., Broyde, S., Geacintov, N. E., and Patel, D. J. (1999) *Biochemistry 38*, 10831−42.
65. Yeh, H. J., Sayer, J. M., Liu, X., Altieri, A. S., Byrd, R. A., Lakshman, M. K., Yagi, H., Schurter, E. J., Gorenstein, D. G., and Jerina, D. M. (1995) *Biochemistry 34*, 13570−81.
66. Geacintov, N. E., Cosman, M., Hingerty, B. E., Amin, S., Broyde, S., and Patel, D. J. (1997) *Chem. Res. Toxicol. 10*, 111−46.

BI002543R